Microscopic Raman Mapping of Epitaxial Graphene on 4H-SiC(0001)

Ryong-Sok O*, Atsushi Iwamoto, Yuki Nishi, Yuya Funase, Takahiro Yuasa, Takuro Tomita, Masao Nagase, Hiroki Hibino[1], and Hiroshi Yamaguchi[1]

Graduate School of Advanced Technology and Science, The University of Tokushima, Tokushima 770-8506, Japan

[1]NTT Basic Research Laboratories, Nippon Telegraph and Telephone Corporation, Atsugi, Kanagawa 243-0198, Japan

Abstract

We propose a quality control method for wafer-scale epitaxial graphene grown on SiC substrates. The peak position of Raman spectra of epitaxial graphene is an excellent indicator of film quality and reveals irregularities, such as graphene thickness inhomogeneity and SiC substrate defects. A comparison of microscopic Raman maps and scanning probe microscopy images of the same position of the sample revealed that wave numbers of Raman peaks (G and 2D band peaks) were strongly correlated with the strain in the graphene film. The increase in number of graphene layers (2 to 3-4 layers) induced phonon softening (~6 cm^{-1}) and broadening (~6 cm^{-1}) of the 2D band peak. Significant phonon softening and abnormal broadening of the Raman peaks were observed at residual scratches on the SiC substrate. The quantitative layer number distribution of graphene on SiC is successfully estimated from the wave number distribution of the 2D band peak.

***E-mail address: oryonsoku@ee.tokushima-u.ac.jp**

1. Introduction

Graphene has attracted tremendous interest in recent years because of its novel electrical properties,[1-3] which make it a promising candidate for future electronic materials. Single-layer and few-layer graphene are commonly fabricated by the mechanical exfoliation method.[1-2] However, graphene flakes are unsuitable for electronic applications because of their extremely small size. Graphene epitaxially grown by the thermal decomposition of SiC under vacuum or argon pressure is expected to be useful as a post-silicon material. Wafer-scale growth and device fabrication of graphene have already been demonstrated.[4-10]

A reliable method for characterization of epitaxial graphene and its quality control on a wafer-scale range is necessary for improving the reproducibility of epitaxial graphene growth. Scanning probe microscopy (SPM) and low-energy electron microscopy (LEEM) are powerful methods for evaluating the film thickness distribution and the surface morphology of epitaxial graphene grown on a SiC substrate.[11-15] However, these methods cannot reveal the strain distribution in graphene as induced by the internal stress of the SiC substrate.[16] The origin of the strain in epitaxial graphene is attributed to the difference in the thermal expansion coefficients between epitaxial graphene and the SiC substrate.[16,27] It has been reported that the strain in graphene influences its electronic properties,[17-18] and results in variation of the graphene film quality. Hence, the strain in epitaxial graphene on SiC must be observed for achieving its quality control.

Microscopic Raman spectroscopy is an important nondestructive method for investigating the physical properties of graphene.[19-22] In particular, this method has proven to be a powerful one for probing the uniaxial or biaxial strain in graphene.[23-26] It has been reported that the phonon hardening of Raman peaks (G and 2D band peaks) for epitaxial graphene grown on SiC is induced by the compressive strain that originates from the high-temperature annealing.[27-29] Moreover, phonon softening is observed with increasing graphene thickness.[27] These phenomena are important for characterizing epitaxial graphene on SiC from the Raman spectra.

However, the spatial distribution of strain induced by the thermal stress of large-scale epitaxial

graphene on the SiC substrate has not been investigated thus far. For the characterization of large-scale epitaxial graphene on SiC, the strain distribution must be analyzed quantitatively and the relationship between the surface morphology and the strain in graphene must be determined by a fixed point observation made by a combination of SPM and microscopic Raman spectroscopy. In this paper, we present the results of microscopic Raman mapping and SPM performed at the same position of few-layer epitaxial graphene on a SiC substrate.

2. Experimental Procedure

We used few-layer epitaxial graphene grown on a semi-insulating 4H-SiC(0001) substrate in an ultra high vacuum (UHV) environment as the sample. The annealing temperature was approximately 1320 °C. It was confirmed by LEEM that a major part of the sample surface (approximately 80%) was covered with bi-layer graphene and the rest was covered with 3 or 4 layer graphene.

Microscopic Raman spectra were obtained at room temperature by using a micro-Raman spectrometer (Renishaw InVia Reflex) equipped with a 100x objective and a scanning stage. The wavelength of the Raman excitation was 532 nm. Scattered light was introduced into a polychrometer and detected by a charge-coupled device (CCD) camera. The scanning step in the microscopic Raman mapping was 0.6 μm. The typical collection time for the point-mode measurement was 10 s/point, and that for the map mode was 5 s/point.

For analyzing the Raman spectra, we obtained the positions and full-width at half maximum (FWHM) of the G and the 2D band peaks[19-22)] by the peak fitting method. The Raman spectra of epitaxial graphene on SiC contained signals that originated from the SiC substrate around the G band peak, as shown in Fig. 1(a). For analyzing the G band peak measured in the point-mode, the background signal from the SiC substrate was removed by a numerical subtraction method. Unfortunately, in the map-mode measurements, a high background level around the G peak prohibited quantitative analysis. In contrast, 2D band peaks measured in the map-mode had

sufficient quality for Gaussian fitting, as shown in Fig. 1(b). Raman map images were generated from the measured data of the 2D band peak position and FWHM. The graphene film thickness and the surface morphology at the same position which measured by the micro-Raman spectrometer were observed by SPM (Veeco Dimension 3100) in the tapping mode. In the LEEM observation, 3 and 4 layer graphene regions could be clearly distinguished. However, in SPM topographic and phase images, it was impossible to clearly distinguish between the 3 and 4 layer graphene. In the results section, the bright island regions in the SPM phase image are clarified as being 3-4 layers graphene.

3. Results and Discussion

3.1 Surface morphology and Raman maps obtained at the same position.

Figure 2 shows the results of the SPM measurements and the microscopic Raman mapping performed at the same position of the sample surface. In the SPM phase image [Fig. 2(c)], bi-layer graphene regions were observed as a dark background, and 3-4 layers graphene regions were observed as bright islands. The irregularities (V shape) seen in the SPM height image [Fig. 2(d)] were residual scratches that remained on the substrate surface after the polishing process. We drew a sketch of the specific surface morphology such as graphene thickness distribution and scratches, as shown in Fig. 2(e). In the Raman map image of the 2D band peak position [Fig. 2(a)], the 3 or 4 layer graphene and the scratch regions were observed as dark contrasts (these regions had a lower wave number than the surrounding area), whereas in the Raman map image of the 2D band peak FWHM [Fig. 2(b)], they were observed as bright contrasts (the FWHM of the 2D band peaks broadened). The dominant regions seen as the bright contrasts in the Raman map image of the 2D band peak position and the dark contrasts seen in the Raman map image of the 2D band peak FWHM corresponded to bi-layer graphene regions. The locations of each of the graphene islands (3-4 layers graphene) and scratches observed on the microscopic Raman map images and SPM images were in good agreement.

3.2 Microscopic Raman measurements in point-mode on each kind of graphene.

For a more detailed analysis, point-mode measurements were carried out at the marked positions shown in Fig. 2(e), where the film quality (bi-layer graphene, 3 or 4 layer graphene, scratch) was confirmed by the SPM observations.

Figure 3(a) shows plots of the position versus FWHM of 2D band peaks in the microscopic Raman spectra obtained by the point-mode measurements for bi-layer graphene (square), 3-4 layers graphene (diamond) and scratch (triangle) regions. Figure. 3(b) shows the typical spectrum of the 2D band peaks for each region. On the bi-layer graphene domains, the 2D band peaks could be divided by four Lorentzian peaks with the FWHM of 35 cm^{-1}, as reported in the literature.[20-22)] In the 3-4 layers graphene and scratch regions, the peaks were symmetrical unlike those in the case of the bi-layer and, they could not be divided by four Lorentzian peaks. As shown in Fig. 3(b), single Gaussian peaks were used for fitting the peaks of the 3-4 layers graphene and the scratch regions. The 2D band peaks obtained on bi-layer and 3-4 layers graphene were observed mainly around wave numbers 2742 cm^{-1}, and 2736 cm^{-1}, respectively. Similarly, the typical values of FWHM were 60 cm^{-1} for bi-layer graphene, and 66 cm^{-1} for 3-4 layers. The FWHM broadening of the 2D band peaks and its magnitude were in agreement with the results reported in ref.22.

However, the positions and FWHM of the 2D band peaks obtained on the scratches varied irregularly. Moreover, relatively significant phonon softening and abnormal FWHM broadening of the 2D band peaks were observed as compared to those in the other regions. From the results shown in Figs. 2(a) and (b), it can be concluded that significant phonon softening of peak positions and abnormal FWHM broadening of Raman peaks reflected surface irregularities such as scratches or defects of SiC at the focal points of Raman measurements. Surface irregularities, such as very small step-terrace structures of the SiC substrate, should be the cause of the irregular growth of graphene. An inhomogeneity of graphene thickness and strain would lead to abnormal Raman spectra. A large peak position shift and abnormal FWHM broadening in the Raman spectra of graphene on the SiC

substrate signified film defects.

3.3 Phonon hardening or softening of G and 2D band peaks.

The phonon hardening or softening of the G and the 2D band peaks was investigated because it is an excellent indicator of the change in the strain in the graphene film.[23-25] We investigated the relationship between the positions of the G and the 2D band peaks on the Raman spectra of epitaxial graphene and compared the results with the theoretically predicted phonon hardening of both the peaks under biaxial strain of exfoliated graphene.

Figure 4 shows plots of the G and 2D band peak positions. The dashed lines represent the calculated results of the phonon hardening in the exfoliated bi-layer and the 3-4 layers graphene under biaxial strain.[24-26] The Gruneisen parameter γ_{mode} (the mode corresponding to the G or the 2D band) in the calculation was defined as

$$\gamma_{mode} = -\frac{1}{\omega_o}\frac{\partial \omega}{\partial \varepsilon_{\parallel}}. \qquad (1)$$

where $\varepsilon_{\parallel}$ is the biaxial strain of graphene and ω_0 and ω are the Raman frequencies at zero strain and under finite strain, respectively. ω_o of bi-layer and 3-4 layers graphene were determined from the typical Raman spectra obtained in the case of exfoliated graphene in ref. 22. The peak positions of bi-layer graphene were determined to be 1582 cm^{-1} for the G band and 2687 cm^{-1} for 2D band. For determining the origins of the Raman peaks for 3 and 4 layer graphene, the same peak positions were used (1581.5 cm^{-1} for the G band, 2695 cm^{-1} for the 2D band). The Gruneisen parameter was 1.8 for the G band peaks and 2.7 for 2D band peaks according to ref. 24.

As shown in Fig. 4, the measured peak positions of the bi-layer, 3 layer, and 4 layer graphene agreed well with the calculated positions. The results suggested that for both bi-layer and 3-4 layers graphene, the internal strain was the major cause of phonon hardening. In bi-layer graphene, the average positions of the Raman peaks were 2742 ± 1.5 cm^{-1} for the 2D band and 1603 ± 0.7 cm^{-1} for the G band. For 3-4 layers graphene, the average positions of the Raman peaks fitted by a

theoretical line were 2736 ± 2.0 cm^{-1} for the 2D band and 1597 ± 1.3 cm^{-1} for G band. The compressive strain estimated from the phonon hardening for bi-layer graphene was 0.73 ± 0.03% and that for 3-4 layers graphene was 0.56 ± 0.05%. This result indicated that an increase in the number of graphene layers induced the stress relaxation.

For the scratch regions, the relationship of peak positions between G and 2D could also be explained by the phonon hardening caused by the strain. In this region, the amount of stress relaxation was larger than that in the bi-layer and 3-4 layers graphene regions. The average compressive strain of the scratch regions in Fig. 4 was 0.2%, which was approximately one-third of that of the non-scratch regions. The reasons for the abnormal broadening of the FWHM of scratch regions were the inhomogeneity of the stress relaxation and the small domains whose size was below the resolution of Raman optics. As a result, defects of graphene as shown in Figs. 2(a) and (b) were clearly observed in the Raman map images. The results of the relationship between the peak position of the 2D band and the G band (Fig. 4) suggests that the scratch regions contained both the components of bi-layer and 3-4 layers graphene.

3.4 Strain distribution on wafer-scale epitaxial graphene film.

As shown in Fig. 4, the peak positions of graphene grown on SiC were an excellent indicator of the compressive strain that induced the phonon hardening. It is considered that the strain distribution on the epitaxial graphene film can be estimated by analyzing the Raman map with respect to the positions of the Raman peaks. Figure 5(a) shows plots of the peak positions versus FWHM of the 2D band peaks obtained by the microscopic Raman measurements of the non-scratch regions. In Fig. 5(a), gray circles represent the map-mode measurements, and squares and diamonds indicate the point-mode measurements of the bi-layer and 3-4 layers graphene, respectively.

Figure 5(b) shows the histogram of the peak positions of the 2D band of the result shown in Fig. 5(a). This histogram was divided into two components by fitting analysis. The average values of the positions and the area ratios of the components were 2743 ± 2.21 cm^{-1} and 81%, respectively, for a

relatively high wave number and 2738 ± 4.53 cm^{-1} and 19%, respectively, for a relatively low wave number. This result was consistent with the result of the LEEM measurement that approximately 80% of the sample surface was covered with bi-layer graphene. The strain of each component and its deviation (strain distribution) corresponded to 0.77 ± 0.03% for the bi-layer graphene and 0.59 ± 0.06% for 3-4 layers graphene. These strain values were estimated from Raman mapping measurements and agreed well with those estimated from the point-mode measurements described in the previous section. Since the typical domain size of 3-4 layers graphene is smaller than the spatial resolution of Raman optics, the further experiments with higher spatial resolution are required to investigate the cause of the inhomogeneity of the layer numbers and strain.

The origin of compressive strain in epitaxial graphene on SiC is attributed to the large difference in the coefficients of linear thermal expansion between SiC[30] and graphene.[16] As described in ref. 16, in epitaxial graphene grown on the SiC surface, a large compressive strain would develop upon cooling. The estimated compressive strain of graphene on SiC for a 1320 °C annealed sample was 0.85% at room temperature. In this case, we used the theoretical coefficient of the thermal expansion of graphene.[31] The difference in thermal expansion coefficients between graphene (2D) and graphite (3D) was almost constant and was approximately 2×10^{-6} K^{-1} for the entire temperature range, as shown in ref. 31. If we used the thermal expansion coefficient of graphite[31] for the graphene layer, the strain was reduced to 0.55%. The residual strain in bi-layer graphene of our samples was slightly smaller than that of ideal graphene. Further, the strain of 3-4 layers graphene was almost the same as that of graphite. These results suggest that as the number of layers increased, the thermal expansion coefficient varied from a two-dimensional value to a three-dimensional one. A more precise estimation is required for the quantitative evaluation of the thermal expansion coefficient. In particular, we have not taken into account the effect of carrier doping from the substrate[32-33]. Further experiments for the growth temperature dependence and substrate doping effect are required.

4. Conclusions

In summary, SPM observations and microscopic Raman mapping measurements were performed at the same position of epitaxial graphene on SiC. The peak position and FWHM of the Raman peak were strongly related to the number of graphene layers and the surface morphology, e.g., defects on SiC. The magnitudes of phonon hardening were attributed to the thermal compressive strain and they were quantitatively estimated for the bi-layer and 3-4 layers graphene grown on SiC. Remarkable random strain relaxation was observed in the scratch (defect) regions. The thickness distribution was successfully estimated from the Raman mapping measurements. Quantitative analysis of the distribution of the Raman peak position is useful for the characterization or quality control of graphene epitaxially grown on SiC.

Acknowledgements

This study was partially supported by Grants-in-Aid for Scientific Research (Nos. 22310086, 20246064, and 21246006) from the Ministry of Education, Culture, Sports, Science and Technology of Japan.

References

1) K. S. Novoselov, A. K. Geim, S. V. Morozov, D. Jiang, Y. Zhang, S. V. Dubonos, I. V. Grigorieva, and A. A. Firsov: Science **306** (2004) 666.

2) K. S. Novoselov, A. K. Geim, S. V. Morozov, D. Jiang, M. I.Katsnelson, I. V. Grigorieva, S. V. Dubonos, and A. A. Firsov: Nature **438** (2005) 197.

3) A. H. Castro Neto, F. Guinea, N. M. R. Peres, K. S. Novoselov, and A. K. Geim: Rev. Mod. Phys. **81** (2009) 109.

4) C. Berger, Z. Song, X. Li, X. Wu, N. Brown, C. N. D. Mayou, T. Li, J.Hass, A. N. Marchenkov, E. H. Conrad, P. N. First, and W. A. de Heer: Science **312** (2006) 1191.

5) M. L. Bolen, S. E. Harrison, L. B. Biedermann, and M. A. Capano: Phys. Rev. B **80** (2009) 115433.

6) V. Borovikov, and A. Zangwill: Phys. Rev. B **80** (2009) 121406.

7) J. Hass, W. A. Heer and E. H. Conrad: J. Phys.: Condens. Matter **20** (2008) 323202.

8) Luxmi, N. Srivastava, G. He, R. M. Feenstra, and P. J. Fisher: Phys. Rev. B **82** (2010) 235406.

9) S. Tanabe, Y. Sekine, H. Kageshima, M. Nagase, and H. Hibino: Jpn. J. Appl. Phys. **50** (2011) 04DN04.

10) S. Tanabe, Y. Sekine, H. Kageshima, M. Nagase, and H. Hibino: Appl. Phys. Express **3** (2010) 075102.

11) H. Hibino, H. Kageshima, F. Maeda, M. Nagase, Y. Kobayashi, and H. Yamaguchi: Phys. Rev. B **77** (2008) 075413.

12) H. Hibino, S. Mizuno, H. Kageshima, M. Nagase, and H. Yamaguchi: Phys. Rev. B **80** (2009) 085406.

13) M. Nagase, H. Hibino, H. Kageshima, and H. Yamaguchi: Appl. Phys. Express **3** (2010) 045101.

14) M. Nagase, H. Hibino, H. Kageshima and H. Yamaguchi: Nanotechnology **20** (2009) 445704.

15) M. Nagase, H. Hibino, H. Kageshima and H. Yamaguchi: Nanotechnology **19** (2008) 495701.

16) N. Ferralis, R. Maboudian, and C. Carraro: Phys. Rev. Lett. **101** (2008) 156801.

17) S.-M. Choi, S.-H. Jhi, and Y.-W. Son: Phys. Rev. B **81** (2010) 081407.

18) S. Kwon, S. Choi, H. J. Chung, H. Yang, S. Seo, S.-H. jhi, and J. Y. Park: Appl. Phys. Lett. **99** (2011) 013110.

19) R. Saito, A. Jorio, A.G. Souza Filho, G. Dresselhaus, M. S. Dresselhaus, and M. A. Pimenta: Phys. Rev. Lett. **88** (2002) 027401.

20) A. C. Ferrari, J. C. Meyer, V. Scardaci, C. Casiraghi, M. Lazzeri, F. Mauri, S. Piscanec, D.Jiang, K.S. Novoselov, S. Roth, and A. K. Geim: Phys. Rev. Lett. **97** (2006) 187401.

21) L. M. Malard, J. Nilsson, D. C. Elias, J. C. Brant, F. Plentz, E. S. Alves, A. H. Castro Neto, and M. A. Pimenta: Phys. Rev. B **76** (2007) 201401.

22) D. Graf, F. Molitor, K. Ensslin, C. Stampfer, A. Jungen, C. Hierold, and L. Wirtz: Nano Lett. **7** (2007) 238.

23) J. E. Proctor, E. Gregoryanz, K. S. Novoselov, M. Lotya, J. N. Coleman, and M. P. Halsall: Phys. Rev. B **80** (2009) 073408.

24) T. M. G. Mohiuddin, A. Lombardo, R. R. Nair, A. Bonetti, G. Savini, R. Jail, N. Bonini, D. M. Basko, C. Galiotis, N. Marzari, K. S. Novoselov, A. K. Geim, and A. C. Ferrari: Phys. Rev. B **79** (2009) 205433.

25) F. Ding, H. X. Ji, Y. H. Chen, A. Herklotz, K. Dorr, Y. F. Mei, A. Rastelli, and O. G. Schmidt: Nano Lett. **10** (2010) 3453.

26) Y. C. Cheng, Z. Y. Zhu, G. S. Huang, and U. Schwingenschlogl: Phys. Rev. B **83** (2011) 115449.

27) J. Rohrl, M. Hundhausen, K. V. Emtsev, Th. Seyller, R. Graupner, and L. Ley: Appl. Phys. Lett. **92** (2008) 201918.

28) Z. H. Ni, W. Chen, X.F. Fan, J. L. Kuo, T. Yu, A.T. S. Wee, and Z. X. Shen: Phys. Rev. B **77** (2008) 115416.

29) M. H. Oliveira, Jr., T. Schumann, M. Ramsteiner, J. M. J. Lopes, and H. Riechert: Appl. Phys. Lett. **99** (2011) 111901.

30) G. Slack and S. Bartram: J. Appl. Phys. **46** (1975) 89.

31) N. Mounet and N. Marzari: Phys. Rev. B **71** (2005) 205214.

32) Y. C. Cheng and U. Schwingenschlogl: Appl. Phys. Lett. **97** (2010) 193304.

33) R. Yang, Q. S. Huang, X. L. Chen, G. Y. Zhang, and H.-J. Gao: J. Appl. Phys. **107** (2010) 034305.

Figure captions

Fig. 1. Typical Raman spectra of bi-layer epitaxial graphene grown on SiC. (a) Raman spectrum around G and 2D band peaks and internal signal of the SiC substrate. (b) Peaks of 2D band obtained by microscopic Raman mapping analyzed in with respect to their position and FWHM by the Gaussian fitting method.

Fig. 2. Microscopic images of epitaxial graphene on 4H-SiC(0001). These were obtained at the same position on the sample surface. Raman map images of positions of (a) 2D band peaks within wave numbers of 2700-2750 cm^{-1} and (b) FWHM in the range 60-75 cm^{-1}. (c) In the SPM phase image, dark contrasts correspond to bi-layer graphene and bright contrasts correspond to 3-4 layers graphene. (d) SPM height image. Residual scratches on the SiC substrate are observed as a small domain of step-terrace structures. (e) Sketch of specific surface morphology on the measured position. The marks (squares, diamonds, and triangles) represent positions of Raman measurements in the point-mode shown in Fig. 3.

Fig. 3. Results of microscopic Raman spectra measurements in the point-mode at the marked points shown in Fig. 2(e). (a) Plots of the peak position versus FWHM of 2D band. (b) Comparison of typical 2D band peaks at each points. The peak of the 2D band obtained on bi-layer graphene was fitted by four Lorentzian peaks with FWHM of 35 cm^{-1}.

Fig. 4. Plots of the positions of 2D band peaks versus positions of G band peaks. The dashed lines represent calculations based on the theory of phonon hardening induced by compressive biaxial strain in ref. 24. The origins (cross marks) of Raman peaks for calculations were 1582 and 2687 cm^{-1} for bi-layer graphene and 1581.5 and 2695 cm^{-1} for 3-4 layers graphene. These values were determined from the typical Raman spectra obtained in the case of exfoliated graphene in ref. 22.

Fig. 5. (a) Plots of the positions versus FWHM of the 2D band peaks obtained by microscopic Raman mapping at the position where only the bi-layer and 3-4 layers graphene domains were observed, and results of Raman measurements in the point-mode. (b) Histogram of peak positions of 2D band at the position where only the bi-layer and 3-4 layers graphene domains were observed. The histogram was split by two Gaussian peaks; the main component was positioned at wave number 2743 ± 2.21 cm^{-1} (bi-layer) and the sub component was positioned at 2738 ± 4.53cm^{-1} (3-4 layers graphene).

Figures (Color)

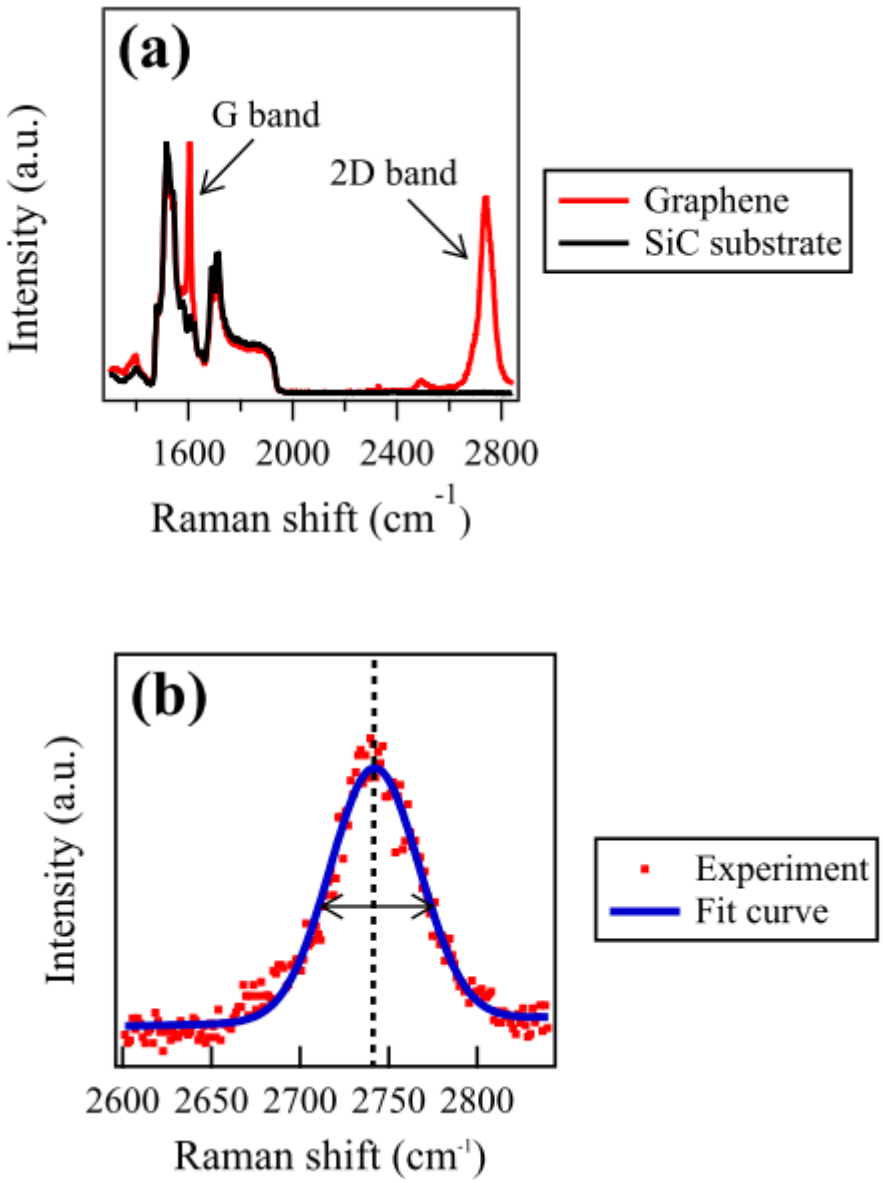

Figure. 1

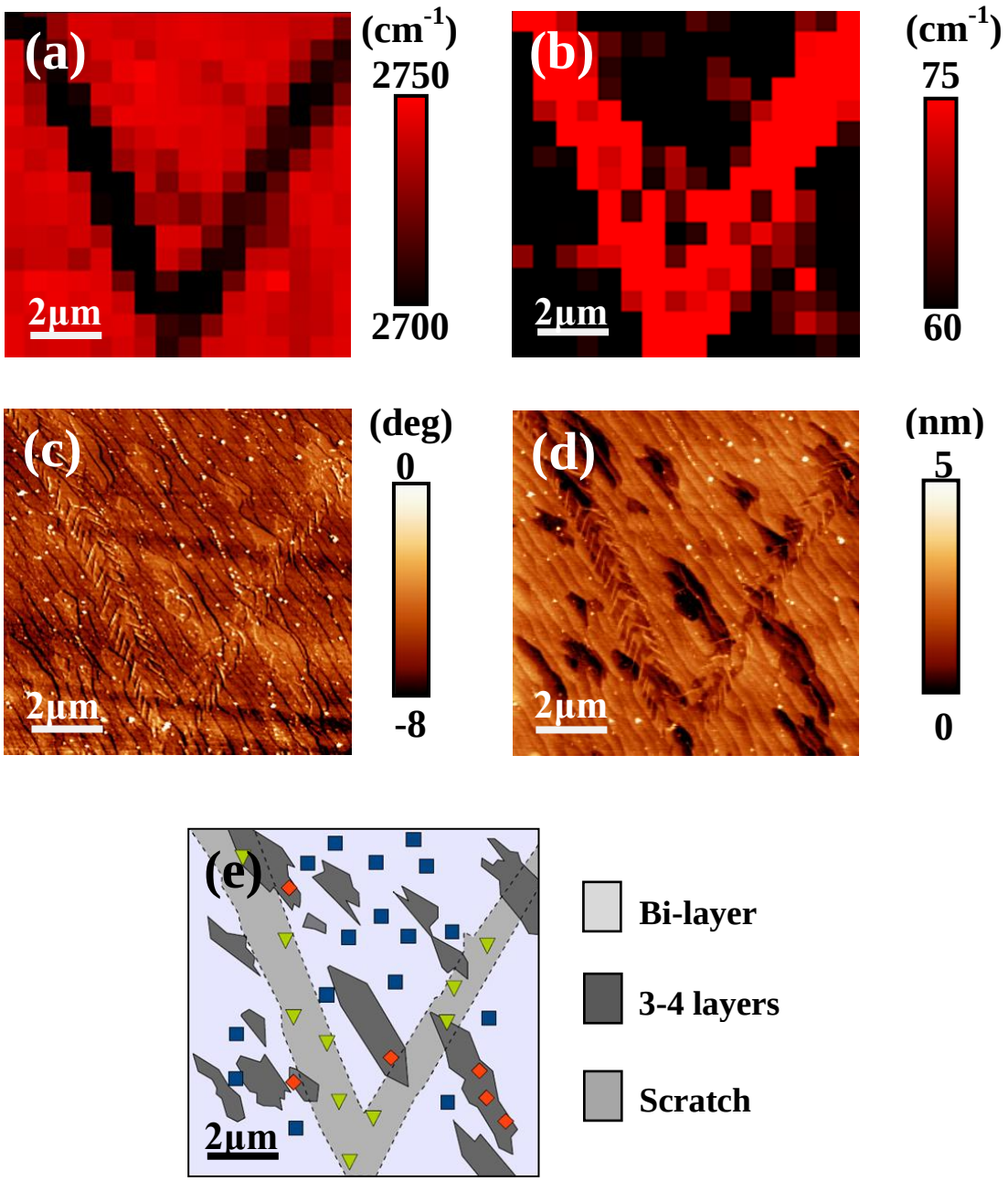
(a)
2µm
(cm-1)
2750
2700
(b)
2µm
(cm-1)
75
60
(c)
2µm
(deg)
0
-8
(d)
2µm
(nm)
5
0
(e)
2µm
Bi-layer
3-4 layers
Scratch

Figure. 2

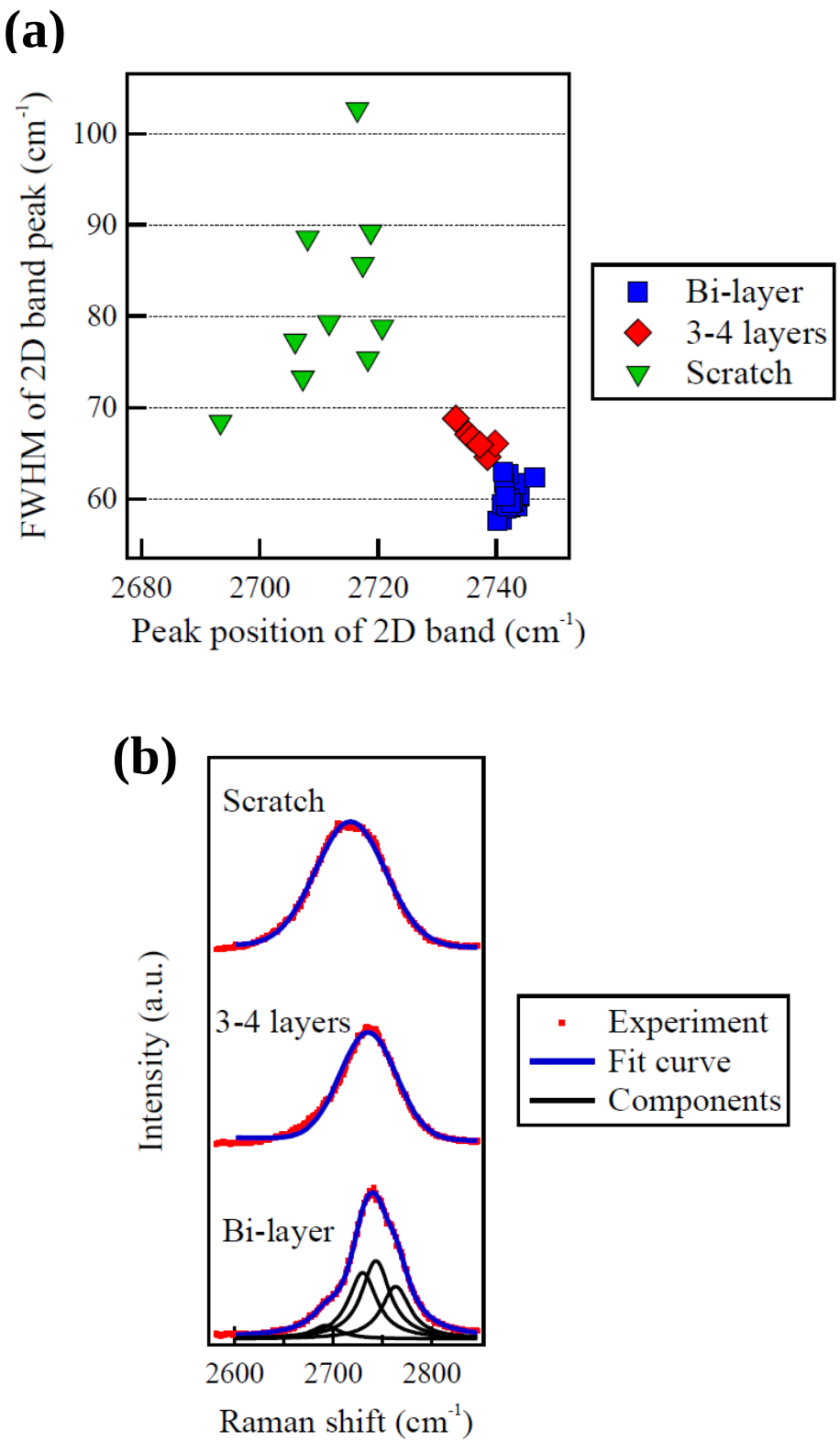
(a)
FWHM of 2D band peak (cm-1)
100
90
80
70
60
2680
2700
2720
2740
Peak position of 2D band (cm-1)
Bi-layer
3-4 layers
Scratch
(b)
Scratch
3-4 layers
Bi-layer
Intensity (a.u.)
2600
2700
2800
Raman shift (cm-1)
Experiment
Fit curve
Components

Figure. 3

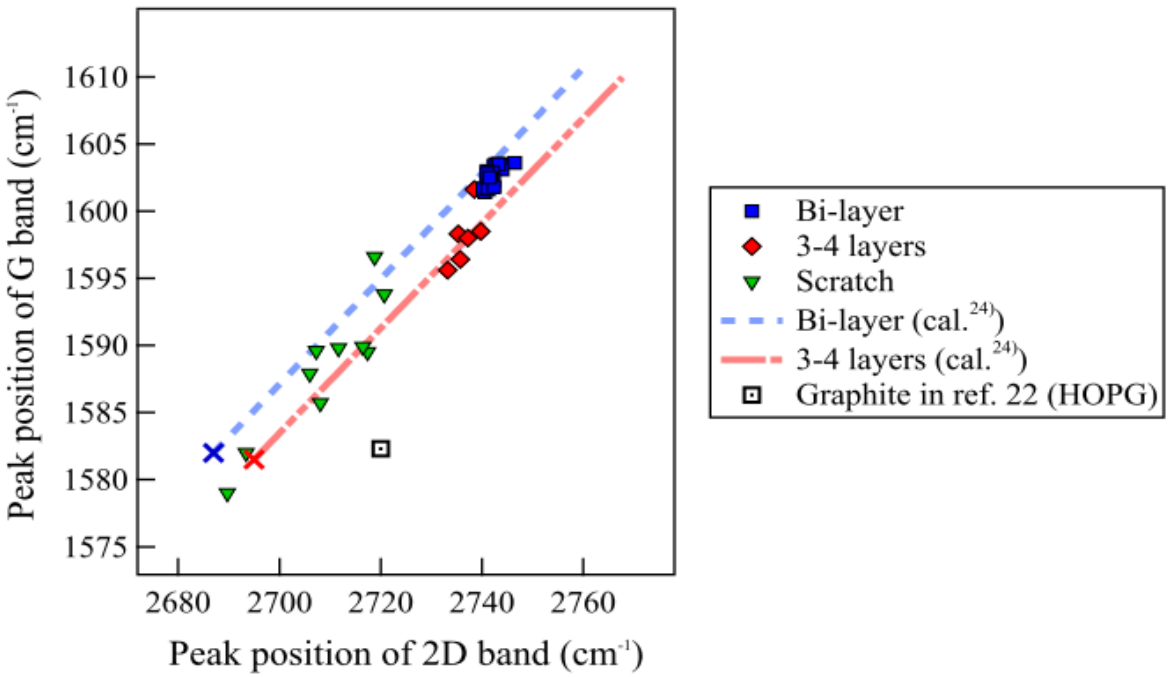
Peak position of G band (cm-1)
1610
1605
1600
1595
1590
1585
1580
1575
2680
2700
2720
2740
2760
Peak position of 2D band (cm-1)
Bi-layer
3-4 layers
Scratch
Bi-layer (cal.[24])
3-4 layers (cal.[24])
Graphite in ref. 22 (HOPG)

Figure. 4

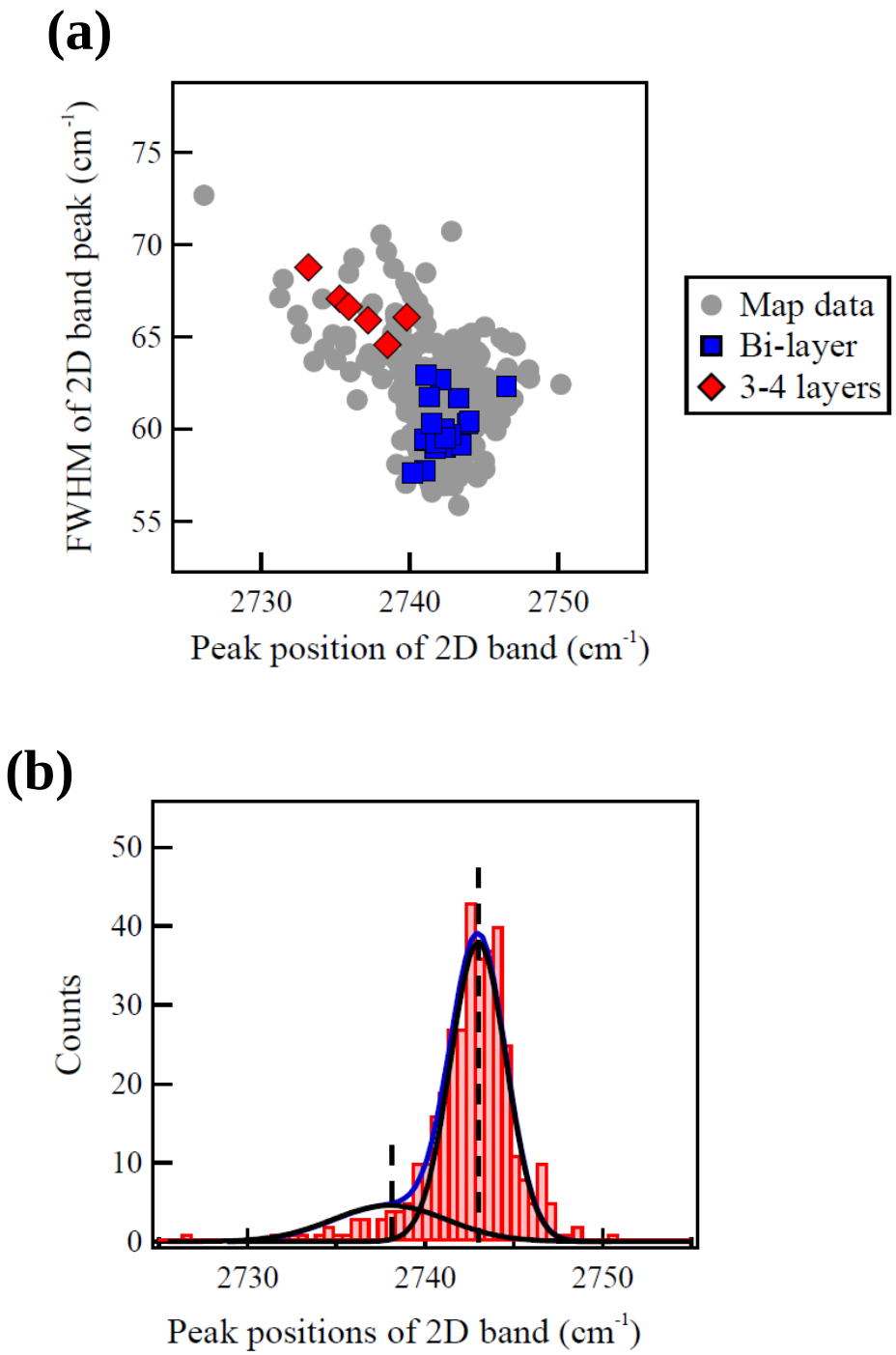
(a)
FWHM of 2D band peak (cm-1)
75
70
65
60
55
2730
2740
2750
Peak position of 2D band (cm-1)
Map data
Bi-layer
3-4 layers
(b)
Counts
50
40
30
20
10
0
2730
2740
2750
Peak positions of 2D band (cm-1)

Figure. 5